

# Cross-Linked Epoxy Composites Filled with Intrinsically Conductive Phthalocyanine Nanocrystals. Influence of Filler Amount, Layer Thickness, and Cross-Linkers Used on the Percolation Threshold and Conductivity Level of the Composites

Zhe Chen,<sup>†</sup> J. C. M. Brokken-Zijp,<sup>\*,‡,§</sup> H. P. Huinink,<sup>‡</sup> J. Loos,<sup>‡,§</sup> G. de With,<sup>‡,§</sup> and M. A. J. Michels<sup>§,‡</sup>

GE China Technology Center, Zhangjiang High Tech Park, Pudong, Shanghai, 201203, PR China; Department of Chemical Engineering and Chemistry and Department of Applied Physics, Eindhoven University of Technology, P.O. Box 513, 5600 MB, Eindhoven, The Netherlands; and Dutch Polymer Institute, P.O. Box 902, 5600 AX, Eindhoven, The Netherlands

Received October 4, 2005; Revised Manuscript Received May 10, 2006

**ABSTRACT:** Novel aquocyanophthalocyaninatocobalt(III) (Phthalcon 11) nanocrystals were used as intrinsically conducting fillers in cross-linked epoxy composites. The prepared conductive composites had a percolation threshold  $\varphi_c$  between 0.9 and 9 vol %. The  $\varphi_c$  appeared to be strongly dependent on layer thickness. Modeling showed that when the layer thickness was sufficiently large the  $\varphi_c$  could be as low as 0.55 vol %. The occurrence of such a low and variable  $\varphi_c$  was explained by the presence of a percolating Phthalcon 11 fractal particle network. Quantitative fractal analysis of these networks indicates that these networks were formed by diffusion-limited cluster–cluster aggregation of the small primary Phthalcon 11 fractal aggregates, which were already present in the Phthalcon 11 powder itself. Moreover, it was found that  $\varphi_c$  and  $\sigma_v$  also strongly depended on the choice of the cross-linker used and on the chosen processing conditions for making the epoxy molecular network, such as cross-linking temperature and gel time. Rheological experiments were done, and models were proposed to explain these unexpected phenomena. The results presented here suggest that also in other thermoset matrices containing other (non)conductive nanoparticles the above-mentioned factors may have a major impact on the final particle distribution in the matrix and therefore on the final material properties of these composites.

## Introduction

Conductive polymer composites are, in general, made by the incorporation of conductive fillers into an insulating polymer matrix. The commercial application of these composites, at present, is rather limited because relatively large amounts of filler are needed to increase the level of conductivity of the polymer matrix.<sup>1,2</sup> It is widely accepted that the conductivity of these conductive polymer composites is based on the presence of a continuous network of (touching) filler particles throughout the matrix. Generally, above a critical filler fraction, the dc volume conductivity  $\sigma_v$  of the polymer composites changes drastically when the filler amount is further increased. This critical filler fraction  $\varphi_c$  is known as the percolation threshold.<sup>3</sup> Many theories were developed to understand such a drastic transition.<sup>4–6</sup> The majority of this literature consists of statistical percolation models, which predict a  $\varphi_c$  at about 15–17 vol % for randomly distributed nonoverlapping hard spheres.<sup>7,8</sup> In conducting polymer composites such a  $\varphi_c$  was sometimes found. However, many researchers managed to achieve much lower ones,<sup>2,9–15</sup> and even  $\varphi_c$  values as low as 10<sup>–2</sup> vol % were reported.<sup>10,11,14,15</sup> In principle, the use of such a low filler amount will be very attractive in practice because it hardly influences the mechanical and processing properties of the polymer matrix itself and even may lead to transparent conductive polymeric

materials. Unfortunately, the factors which account for such a low  $\varphi_c$  are complicated and partly unknown. It has been reported that the properties of the fillers, such as size, aspect ratio, and surface properties, the properties<sup>1,2</sup> of the matrix including viscosity and crystallinity,<sup>1,2</sup> the interfacial energy between the particles and the matrix,<sup>11,12,19</sup> and the quality of the nanoparticle dispersion may influence the percolation threshold.<sup>1,2,11</sup> However, currently only a few models exist which take into account some of these factors and by which some of the experimental results found could be explained.<sup>3,8,16–19</sup>

The morphology of the composite after processing is also important.<sup>1,2,11,19,20</sup> This morphology may be a very complex arrangement of particle aggregates and networks with different size and shape distributions. In some cases these aggregates/networks exhibit a self-similarity when the scale of observation is changed (fractal network structures).<sup>11,14,15,21</sup> Another problem is that the networks may be distributed in an inhomogeneous way through the matrix.<sup>22</sup>

Fractal network geometry is closely related to percolation theory and, at present, is sometimes used to quantify the particle network morphological features of conducting polymer composites.<sup>14,15,23</sup> Fractal geometry was initially developed by Mandelbrot,<sup>24</sup> and at present, the theory of fractal structures is extensively employed in many branches of physics, chemistry, and mechanics.<sup>25,26</sup> This theory makes it possible to quantitatively describe the structure of various disordered particle aggregates via their fractal parameters. It also helps to explain the occurrence of an extremely low percolation threshold  $\varphi_c$  for some conductive polymer composites.<sup>11,14,15</sup>

Almost all publications on conductive polymer composites containing (semi) conductive fillers are focusing on thermo-

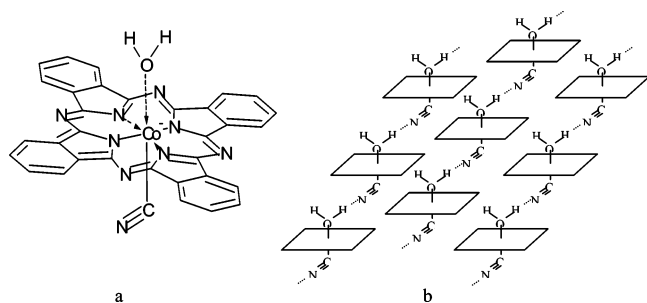
<sup>†</sup> GE China Technology Center.

<sup>‡</sup> Laboratory of Materials and Interface Chemistry, Eindhoven University of Technology.

<sup>§</sup> Dutch Polymer Institute.

<sup>‡</sup> Department of Applied Physics, Eindhoven University of Technology.

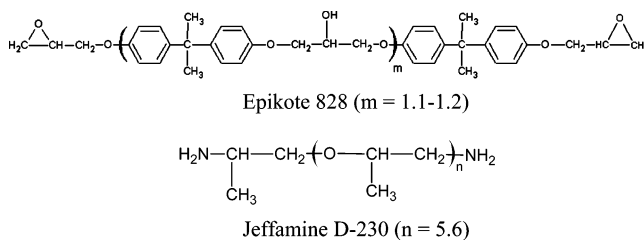
\* Corresponding author: e-mail j.brokken@tue.nl; Fax +31 40 2445619; Tel +31 40 2473742.

**Scheme 1. Molecular Structure (a) and Crystal Structure (b) of Aquocyanophthalocyaninatocobalt(III) (Phthalcon 11)**

plastic polymer matrices.<sup>1,2</sup> It has been shown that the nanocrystals of aquocyanophthalocyaninatocobalt(III) (Phthalcon 11) can be used as a semiconductive additive in a broad range of thermoplastic polymer matrices.<sup>13,28</sup> All these materials are characterized by a very low  $\varphi_c$ .<sup>13,28</sup> We here describe the use of Phthalcon 11 as semiconductive filler in cross-linked epoxy polymer matrices. Thermosets with (semi)conductive nanoparticles are of practical interest, for instance, in static dissipative flooring, (semi)conductive adhesives, and thin transparent electrodes. In this article the focus is on cross-linked epoxy as matrix. It has been shown earlier that a semiconductive homogeneous thin Phthalcon 11/epoxy layer can be made with a low percolation threshold.<sup>22</sup> This low percolation threshold was explained by the formation of a fractal particle network because of the large surface tension difference between particle and matrix.<sup>22</sup> We here describe that also other factors may have a large influence on the  $\varphi_c$  and  $\sigma_v$  of cross-linked Phthalcon 11/epoxy materials. Special attention will be given to the fractal characteristics of the Phthalcon 11 particle network and the way these networks are formed, to the dependence of the  $\sigma_v$  and  $\varphi_c$  and the particle network morphology on the chosen  $M_w$  of the cross-linker used, on the role of the solvent present, on the processing conditions used, and on the layer thickness obtained. Several models will be proposed to explain these unexpected results. The impact of our findings on other cross-linked polymer composites containing nanoparticles will also be discussed.

## Experimental Section

**A. Materials.** Phthalcon 11 (Scheme 1) was synthesized in high purity and yield using a two-step reaction, as was described before.<sup>13,22,28</sup> The Phthalcon 11 powder obtained is highly crystalline, and the primary particle size of Phthalcon 11 as used here is about 150 nm in length and width and about 40 nm in thickness. The unit cell of this compound is monoclinic  $P2_1$  with lattice parameters  $\beta = 102.59^\circ$ ,  $a = 7.308 \text{ \AA}$ ,  $b = 24.89 \text{ \AA}$ , and  $c = 7.149 \text{ \AA}$ .<sup>13</sup> Phthalcon 11 has the proposed molecular and crystal structure of (Scheme 1). This structure was confirmed by FT-IR, proton, <sup>13</sup>C solid and liquid NMR, pyrolysis combustion mass spectrometry, neutron, electron, and X-ray diffraction, XPS, and labeling of the specific groups in the molecule (<sup>2</sup>D<sub>2</sub>O and <sup>13</sup>CN).<sup>28</sup> When these molecules are arranged according to Scheme 1b, the crystals are semiconductive without specific doping.<sup>27,28</sup> The powder dc volume conductivity determined under pressure at room temperature is about  $10^{-4} \text{ S/cm}$ , and the intrinsic conductivity of the crystals  $\sigma_0 = 0.02 \text{ S/cm}$ .<sup>27</sup> Phthalcon 11 has an excellent stability in air, in moisture, and in contact with a broad range of solvents.<sup>28</sup> Phthalcon 11 decomposes at a temperature above 330 °C before melting, and it has attractive health, safety, and environmental properties.<sup>28</sup> The diglycidyl ether of bisphenol A used (Epikote 828, Scheme 2) was a product of Resolution Nederland BV. The bifunctional primary amine cross-linkers used, Jeffamine D230, D400, and D2000, have a  $M_w$  of 230, 400, and 4000, respectively (Scheme 2). They were purchased from Huntsman. *m*-Cresol (pA) was purchased from Merck. All of these compounds were used as received.

**Scheme 2. Chemical Structures of the Prepolymer Components Used To Make the Cross-Linked Epoxy Materials**

**B. Epoxy Composite Preparation.** For the cross-linked Phthalcon 11/epoxy composites a preparation method was used, which led to a homogeneous material even when the layer thickness was as low as 10  $\mu\text{m}$ .<sup>22</sup> First, the dried Phthalcon 11 powder was dispersed in *m*-cresol. To this dispersion Epikote 828 and Jeffamine cross-linker were added ( $\text{NH}_2/\text{epoxy} = 0.5$ ; this ratio is the molar ratio of the  $\text{NH}_2$  and epoxy groups present in the prepolymer formulation before cure). This mixture was magnetically stirred, ultrasonically degassed, and casted on a polycarbonate substrate with a square applicator. Generally, the layer was cross-linked at 100 °C for 4 h and postcured at 120 °C for 24 h under vacuum. Cross-linked Phthalcon 11/epoxy layers with a thickness between 9 and 200  $\mu\text{m}$  were made containing Phthalcon 11 concentrations between 0 and 20 wt %. This weight percentage is based on the total composite composition after cross-linking. The vol % was calculated by taking into account the densities of Phthalcon 11<sup>13,28</sup> and cross-linked epoxy of respectively 1.65 and 1.00  $\text{g/cm}^3$ . The thickness of the cross-linked layers was determined using a digital tip micrometer. Sufficient colloidal stability was always obtained for this composite component mixture in order to avoid phase separation before or during cross-linking.<sup>22</sup> A more detailed description how these materials were made is given in ref 22.

A few thin layers were made without using *m*-cresol for comparison reasons as follows: Phthalcon 11 was dispersed directly into the Jeffamine cross-linker used. The dried Phthalcon 11 powder was dispersed in the Jeffamine cross-linker using magnetic stirring at 40–60 °C. Then it was ultrasonically dispersed at room temperature for 1 h. Then Epikote 828 was added under mechanical stirring by maintaining the ( $\text{NH}_2/\text{epoxy} = 0.5$ ; this ratio is the molar ratio of the  $\text{NH}_2$  and epoxy groups present in the prepolymer formulation before cure), and the mixture was ultrasonically degassed. From this dispersion a cross-linked layer was made following the procedure described above. The results of these coatings are shown in Figure 10 ( $\sigma_v$  noncontact technique).

**C. Morphology Characterization, Rheology, and Conductivity Measurements.** The distribution of the particles in the composites was studied by microscopy. Optical microscopic (OM) analysis was carried out with a Carl Zeiss LM Axioplan microscope (Germany) using the transmitted light bright field technique. Electron microscopic analysis was performed with a JEOL 2000FX transmission electron microscope (TEM) using thin cross-sectional cuts of the cured Phthalcon 11/epoxy composites of about 150 nm thick. These were prepared by cryogenic slicing.

The  $\sigma_v$  of the composite layers was generally measured using the standard four-probe technique (ASTM D 991) using conductive silver paint to ensure good contact between the sample surface and the electrodes. A Keithley 237 source was used to provide the constant current, and a Keithley 6517A high resistance voltmeter was used to measure the voltage. The thin layers made from the Phthalcon 11 dispersion in Jeffamine always had an insulating top layer, and therefore the  $\sigma_v$  could not be measured with the four-probe technique described above. To measure the  $\sigma_v$  in the presence of an insulating surface layer, a noncontacting electrostatic method, which was present in the Laboratory of Océ Technologies B.V., The Netherlands, was used. Both methods were used in accordance with the procedures and instructions described in ASTM D991 and Keithley "Low Level Conductivity Measurements". With our four-probe unit  $\sigma_v \geq 10^{-11} \text{ S/cm}$  could be measured for our samples, while with our noncontacting unit  $\sigma_v \geq 10^{-8} \text{ S/cm}$  could be

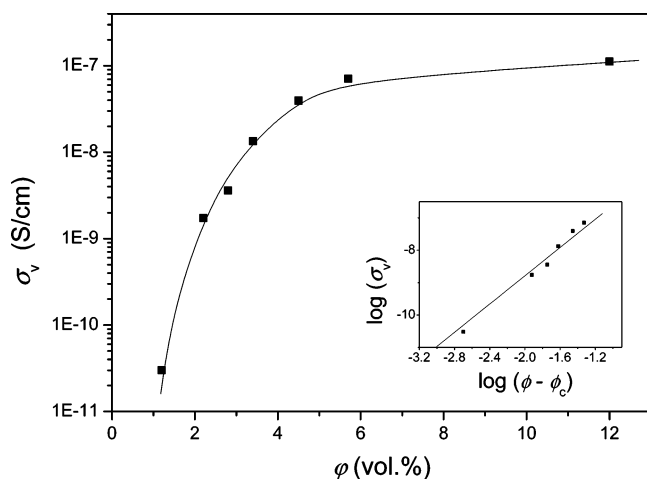


**Figure 1.**  $\sigma_v$  of cross-linked Phthalcon 11/Epikote 828/Jeffamine 230D composites vs the Phthalcon 11 vol %  $\phi$  (method 2). The inset shows the linear relationship between  $\log \sigma_v$  and  $\log(\phi - \phi_c)$  ( $t = 2.1$ ). Layer thickness 150  $\mu\text{m}$ .

measured for our samples. Both values are well above the conductivity of the pure epoxy ( $\sigma_v = 10^{-16}$ – $10^{-17}$  S/cm).<sup>11</sup>

The isolating surface layer was measured using 3-D morphological analysis with the confocal laser scanning microscope in the transition mode (Carl Zeiss LSM 510, Germany).

Rheological measurements were done using an AR1000 rheometer with 12 mm plate–plate geometry. The surface tension measurements were done with a digital tensiometer (KRÜSS K10t, Germany) using the Wilhelmy plate method. The surface tension values obtained for the Jeffamine cross-linkers were within the fault of measurement equal ( $33.4 \pm 0.4$  mN/m). The surface tension values for the Jeffamine/Epikote 828 and Jeffamine/Epikote 828/*m*-cresol mixtures were both equal to those mixtures containing Jeffamine D230 described before.<sup>22</sup>

## Results and Discussion

### A. Low Percolation Threshold and Particle Network

**Analysis.** Phthalcon 11 is a patented novel organic compound developed inside Shell.<sup>13</sup> Its molecular and crystal structure is shown in Scheme 1. The relation between the Phthalcon 11 amount used and the volume conductivity  $\sigma_v$  of the cross-linked epoxy composite is shown in Figure 1. By extrapolating the curve presented here to a  $\sigma_v$  of  $10^{-16}$  S/cm (the conductivity of the pure epoxy matrix<sup>11</sup>), the percolation threshold  $\phi_c$  appeared to be 1.6 wt % or 0.9 vol % (layer thickness 150  $\mu\text{m}$ ; see also below), which is much lower than the theoretical value of  $\sim 16$  vol %.<sup>7,8</sup>

In the inset of Figure 1  $\log \sigma_v$  is plotted as a linear function of  $\log(\phi - \phi_c)$ . This suggests that a percolation type of scaling relation exists between  $\phi$  and  $\sigma_v$ .<sup>8,22,29</sup>

$$\sigma_v = c(\phi - \phi_c)^t \quad (1)$$

where  $c$ ,  $\phi_c$ , and  $t$  are respectively a constant, the percolation threshold, and the conductivity exponent. We found  $t = 2.1$ . This is in good agreement with the theoretical value ( $t = 2.0$ ) predicted for 3D percolating systems.<sup>29,30</sup>

The conductivity of these composites can be explained by the presence of Phthalcon 11 particle networks through the insulating polymer matrix (Figure 2). These particle networks could be observed using OM, confocal laser scanning microscopy (CLSM), and TEM although the size of the primary particles are well below the resolution limit of the first two optical techniques. The structure of these Phthalcon 11 particle networks was studied with OM and TEM at Phthalcon 11

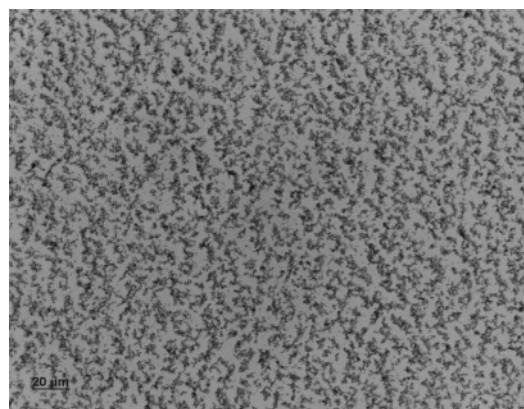


**Figure 2.** Phthalcon 11 (1.8 vol %) particle network in cross-linked Epikote 828/Jeffamine D230 (OM). For details see Figure 1.

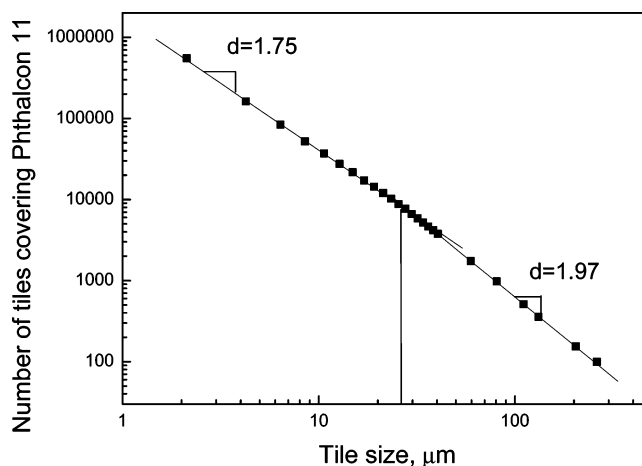


**Figure 3.** Double-logarithmic plot of the number of tiling units covering Phthalcon 11 vs the length scale of the tiling units using the OM data presented in Figure 2.

concentrations just above  $\phi_c$  using as fractal analysis method the method of tiling.<sup>22,25,26</sup>

The counted number of tiles  $N$  in the OM pictures was plotted on a logarithmic scale vs the size  $a$  of these tiles (Figure 3). In this figure it is shown that the number of tiles scales with the tile sizes according to

$$N(a) \propto a^{-d_f} \quad (2)$$

In this equation the exponent  $d_f$  represents the fractal dimension of the aggregates.<sup>31</sup> In Figure 3 two linear regions are observed, which intersect around 20  $\mu\text{m}$ . The slope of the line below 10  $\mu\text{m}$  corresponds to a fractal dimension  $d_f = 1.75$ . When the tile size is larger than 30  $\mu\text{m}$ ,  $d_f = 1.97$  is observed, which is close to the Euclidean dimension ( $D = 2$ ). This indicates that at dimensions above 30  $\mu\text{m}$  the particle network is no longer fractal. We also investigated the fractal structure on a smaller dimension by means of TEM analysis (Figure 4a).

These images were also analyzed with the same tiling method described above (Figure 4b). In this figure the curve fitted through these points also consists of two linear regions. If the size of the tiling units is below 450 nm,  $d_f = 1.41$ . Above 450 nm,  $d_f = 1.78$ , in good agreement with  $d_f = 1.75$  as obtained from the OM images of the same cross-linked composite (size of tiling units below 10  $\mu\text{m}$ ). This suggests that the Phthalcon 11 particle networks after cross-linking contain two fractal aggregate structures and that the larger ones are formed from small primary aggregates ( $d_f = 1.41$ ) during processing.



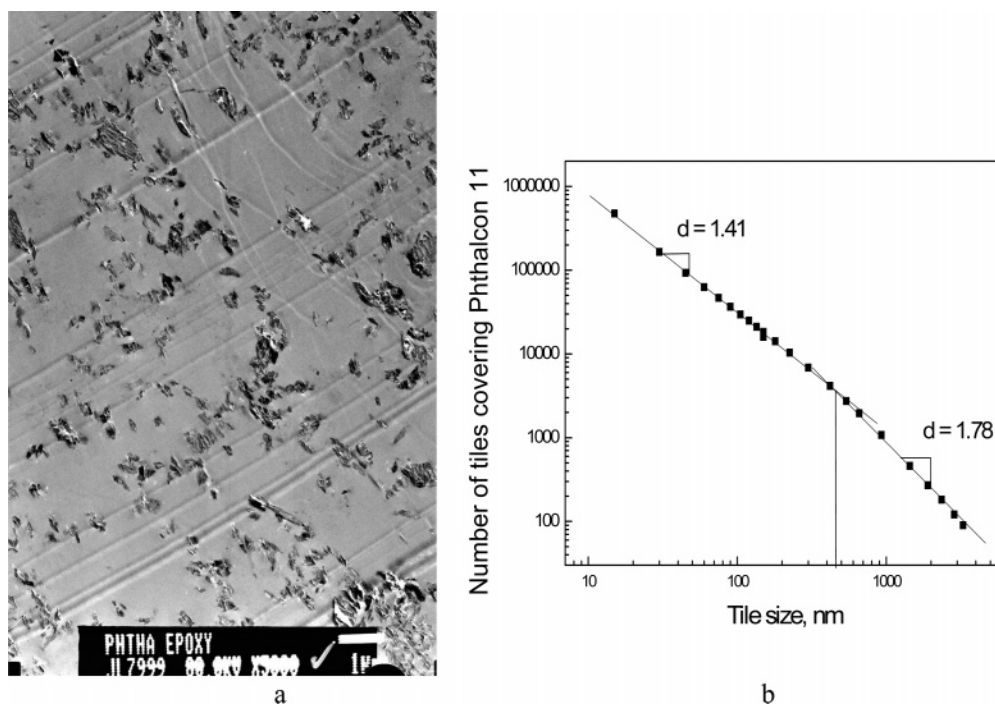


**Figure 4.** (a) TEM image of the material shown in Figure 2; sample thickness 150 nm (same material as in Figure 2). (b) Double-logarithmic plot of the number of tiling units covering Phthalcon 11 vs the length scale of the tiling units using the data of (a).

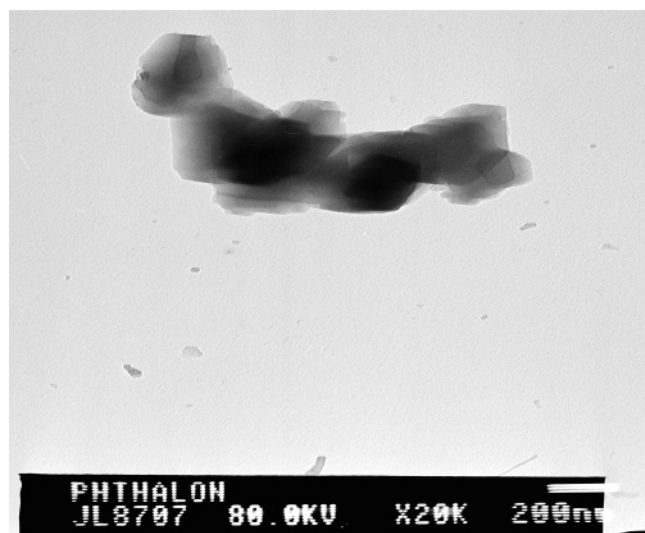


**Figure 5.** Phthalcon 11 primary fractal aggregate (Phthalcon 11 powder; TEM). This powder was used as filler in the cross-linked epoxy composites presented here.

Direct analysis of the Phthalcon 11 powder itself using TEM confirmed this. TEM analysis of the Phthalcon 11 powder indeed showed that the powder consists of small particle aggregates and not of separated primary particles itself (Figure 5). It is likely that these small fractal primary particle aggregates are also present in the prepolymer mixture before cross-linking.

That these primary fractal aggregates were indeed very small in fractal size was confirmed using OM. In the Phthalcon 11/*m*-cresol/Epikote 828/Jeffamine D230 mixtures used to make these layers no particle aggregates/agglomerate structures were detected under the optical microscope. Hence, the process of Phthalcon 11 particle network formation during the cross-linking of the epoxy prepolymer mainly determines the fractal dimension of this network after processing. The  $d_f$  value of 1.75–1.78 found here is close to  $d_f$  value reported for diffusion-limited cluster–cluster aggregation.<sup>32–36</sup> This suggests that the Phthal-

con 11 particle network is formed by diffusion-limited cluster–cluster aggregation (DLA).

The low  $\varphi_c$  found for our cross-linked Phthalcon 11/epoxy composites can be explained by the fractal nature of our primary particle and secondary particle aggregates. It is well-known that both can lower considerably the  $\varphi_c$  of conductive nanofiller polymer matrix composites.<sup>11,14,15,19,21</sup> This can be understood as follows. The percolating network can be considered as a network build of  $N$  spherical building blocks or blobs with radii  $R$  inside a composite volume  $V$ . The volume percentage of these blobs  $p$  can be calculated as follows:

$$p \equiv \frac{4}{3}\pi R^3 N/V \times 100\% \quad (3)$$

It has to be pointed out that for our cross-linked composite materials  $p_c$  and not  $\varphi_c$  is the variable that needs to be used to explain the position of 16 vol % of the percolation threshold determined with the percolation theory. As observed in the OM and TEM studies, the blobs are not inert but have fractal structure itself partly due to DLA type of particle network formation. As a consequence, the actual volume percentage of Phthalcon 11 at the critical filler fraction  $\varphi_c$  can be described by

$$\varphi_c = (a/R)^{3-d_f} p_c \quad (4)$$

In eq 4  $a$  is the radius of the Phthalcon 11 primary aggregate, and the polymer matrix is assumed to be infinite in size in all the three dimensions. Hence,  $\varphi_c$  is much lower than  $p_c$  in relation 4 and much lower than 16 vol %.

The low  $\varphi_c$  shown in Figure 1 was explained before by the strong specific interactions between the surface groups of the Phthalcon 11 particles and the groups present in the dispersing medium and by the strong interactions between the particles itself.<sup>22</sup> These interactions can be quantified using the effective Hamaker constant of particle and matrix component(s), which can be related directly to the interfacial energy between them.

Hence, the large interfacial energy, as is the case in Figure 1, explains also why these fractal networks are formed at such a low concentration and why the  $\varphi_c$  value is below 1 vol % in these materials.<sup>22</sup>

**B. Influence of the Layer Thickness on  $\varphi_c$  and  $\sigma_v$  of Cross-Linked Phthalcon 11/Epoxy Composites.** For conductive polymer composites made from thermoplastic polymers the thickness of the polymer layer is generally large, and no significant influence of layer thickness on the conductive properties is expected. However, in cross-linked polymer layers, the thickness may be much smaller than the other two dimensions. This may influence the fractal particle network structure formation and therefore the  $\varphi_c$  and  $\sigma_v$  of the composite. However, to our knowledge, such an effect was never reported before for polymer nanocomposites. That this influence of layer thickness may exist can be deduced from the model presented above due to a transition of a 3-D into a 2-D particle network structure. Especially when the dimensions of the fractal aggregates from which the final fractal network is formed are large a dependency of  $\sigma_v$  with layer thickness may be observed.

Such an influence of layer thickness may have a major effect on the use of conductive polymer nanocomposites in practice, and therefore we studied these effects in more detail using cross-linked Phthalcon 11/epoxy composites made with variable thickness and Phthalcon 11 concentration. For all these layers  $\sigma_v$  was determined. For a layer thickness between 9 and 150  $\mu\text{m}$   $\varphi_c$  values between 9 and 0.9 vol % were found. The results are shown in Figure 6a. These data show that for most of the Phthalcon 11 concentrations used the  $\sigma_v$  depends strongly on the thickness of the matrix. The thinner the layer, the lower  $\sigma_v$  is. Furthermore, also  $\varphi_c$  clearly increases with decreasing layer thickness  $H$ . To explain this phenomenon, expression 5 for the relationship between  $\varphi_c$  and  $H$  has been derived (see Appendix).

$$\varphi_c \propto C + (H/2R)^{-1/\nu_3} \quad (5)$$

In this expression,  $C$  is a constant and  $\nu_3$  is the correlation length exponent in a 3D system ( $\nu_3 \approx 0.88$ ).<sup>29,37</sup> To test the validity of eq 5, we have plotted in Figure 6b the  $\varphi_c$  as a function of  $(H/2R)^{-1/\nu_3}$  (by extrapolation of the data of Figure 7a). Equation 5 appears to be in reasonable agreement with the data points presented in Figure 6b. Only the percolation threshold of the thinnest film ( $\sim 9 \mu\text{m}$ ) deviates from the solid line. That this particular thin layer deviates can easily be understood because 9  $\mu\text{m}$  is just below the typical size of a DLA aggregate ( $2R \sim 10 \mu\text{m}$ ). Hence, we can conclude that the observed increase in  $\varphi_c$  and the decrease in  $\sigma_v$  with a decrease in  $H$  are due to the fact that the system transfers from a 3D into a 2D system. When  $H$  becomes sufficiently large, the  $\varphi_c$  becomes independent of  $H$  ( $H \rightarrow \infty$ ) and equal to the intercept on the y-axis. Using in eq 5 the values  $R = 5 \mu\text{m}$  and  $d_f = 1.75$  (previous section), the value calculated for the bulk is  $\varphi_c = 0.55 \text{ vol } \%$ . This is slightly lower than the value determined for the 150  $\mu\text{m}$  thick layer of Figure 1, which is in line with the presented data in Figure 6.

Equation 5 can also be used to calculate the ratio  $a/R$  ( $a/R = 0.064$ ). Using  $R = 5 \mu\text{m}$  and this ratio,  $a$  becomes 0.3  $\mu\text{m}$ . This is within the fault of measurement equal to the size of the primary aggregate ( $2a = 0.45 \mu\text{m}$ ) as was independently deduced in the previous chapter, and these results nicely confirm our proposed model.

When  $\varphi$  is above  $\varphi_c$ , the  $\sigma_v$  values are initially strongly dependent on the thickness of the layer until ultimately the  $\sigma_v$  values levels off to a plateau value of about  $1 \times 10^{-7} \text{ S/cm}$  (Figure 6a). This plateau seems to be independent of the layer thickness. Why this is so is being studied at this moment in

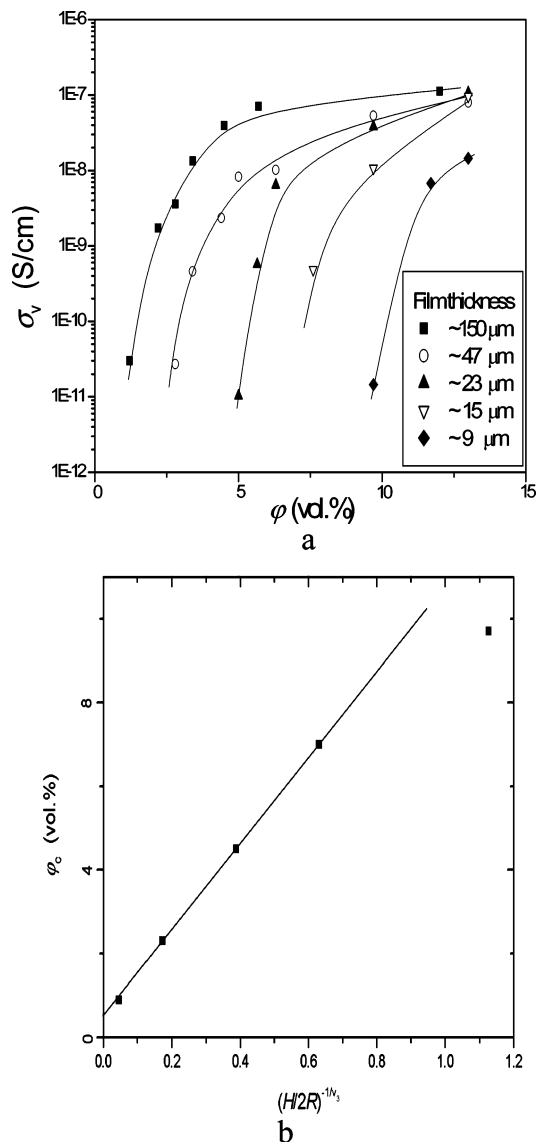


**Figure 6.** Phthalcon 11/epoxy layers cross-linked with Jeffamine D230. (a) The relation between the  $\sigma_v$  and the concentration of Phthalcon 11 ( $\varphi$ ) for different layer thicknesses ( $H$ ). The  $\sigma_v$  was measured using the four-probe method described in the Experimental Section. (b) The relation between the percolation threshold  $\varphi_c$  and the layer thickness ( $H$ ) for the materials presented in (a).

more detail. Below it will be shown that this plateau value is influenced strongly by the molecular weight of the cross-linker used.

All the  $\sigma_v$  data were measured on the top of the layers using a four-probe measuring method that means the current was flowing alongside the top layer. When two probe measuring methods are used that measure the current through the layer thickness, we expect that the influence of layer thickness on  $\sigma_v$  and  $\varphi_c$  will be opposite: the thinner the layer, the lower the percolation threshold and the larger the volume conductivity, and eq 5 has to be modified to forecast this relation quantitatively.

To our knowledge, no experimental information on the influence of layer thickness on  $\varphi_c$  and  $\sigma_v$  in polymer nanocomposites has been published. An interesting review article of V. I. Roldighin and Vysotskii on percolation properties of thin-metal-filled polymer films using micron-sized fillers was published in 2000.<sup>38</sup> They compared two layers with different thickness and reported a lower  $\varphi_c$  for the thinner one. However, the use of much larger micron-sized metal particles (average

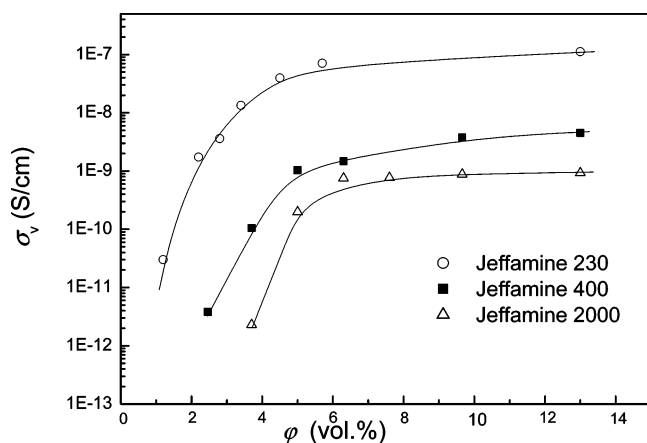


**Figure 7.** Relation between the  $\sigma_v$  and the concentration of Phthalcon 11 ( $\phi$ ). The epoxy composites were cross-linked with different Jeffamine cross-linkers. Processing temperature 100 °C. Layer thickness  $\cong$  150–200 nm.

size 8  $\mu\text{m}$ ), by which it is unlikely that (fractal?) particle networks are formed by Brownian movement via DLA during processing, and the limited amount of experimental detail make a detailed comparison with our results impossible.

The dependency of the  $\sigma_v$  on the direction of measurement in thin nanoparticle polymer layers may have a major impact on the usefulness of these layers in practice.

**C. Influence of the  $M_w$  of the Cross-Linker Used on the Fractal Particle Network Structure and on the  $\log \sigma_v$ – $\phi$  Relation.** The formation of a continuous particle network structure of Phthalcon 11 particles in the cross-linked polymer is, apart from layer thickness, also influenced by the initial

dispersion quality of particle aggregates in the composite component mixture before cross-linking.<sup>22</sup> The influence of the interfacial tension on  $\phi_c$  is expected to be also large when Jeffamine D230 is used as cross-linker because of the large interfacial energy between particles and matrix components for these prepolymer mixtures.<sup>11,22</sup> To see whether other factors may play also a role, Jeffamine cross-linkers with a very similar molecular structure and surface tension but with a different molecular weight  $M_w$ , viz. 230, 400, and 2000, were used for cross-linking the Phthalcon 11/*m*-cresol/Epikote 828 prepolymer under the same processing conditions. As is shown in Figure 7, the  $\sigma_v$  value of the layers cross-linked by Jeffamine D230 reached a plateau of around  $10^{-7}$  S/cm, while for those cross-linked by Jeffamine D400 and Jeffamine D2000, the values of the plateau were only about  $10^{-9}$  and  $10^{-10}$  S/cm, respectively. These data also suggest that the  $\phi_c$  increases with the increase in  $M_w$  of the cross-linker although neither the surface energy of the cross-linker itself nor the surface energy of the total component mixture was influenced by the  $M_w$  variation in Jeffamine (see Experimental Section). As is shown in Figure 8, the optical microscopic images of the Phthalcon 11 fractal particle network structures after processing are also distinctively dependent on the Jeffamine used. The cross-linked layer made with Jeffamine D230 has a particle network of highly ramified fractal aggregates, while in the layer made with Jeffamine D400 or Jeffamine D2000, the fractal aggregates are getting much coarser and denser, which suggests a larger correlation length ( $\xi$ ).

From a structure–property relation point of view, the  $\sigma_v$  may be related to the fractal morphology of a fractal particle network inside the polymer matrix. In general, for a specific system, the particle network may be described as stacked fractal

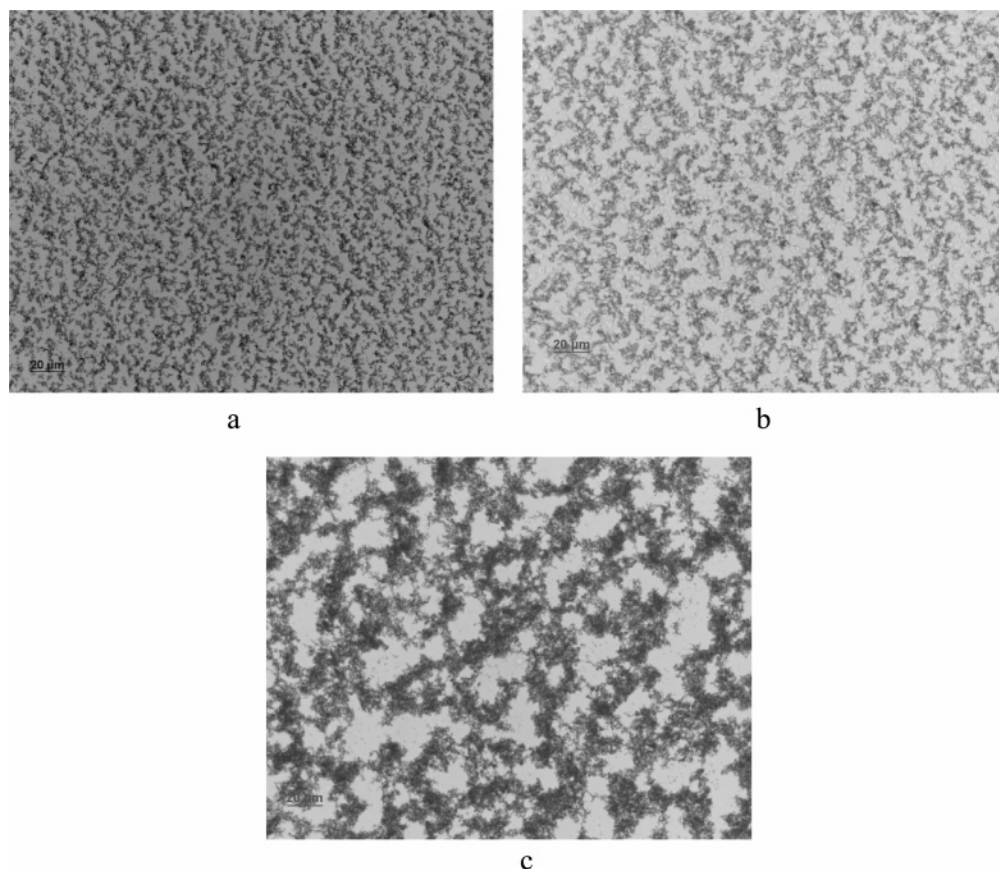


**Figure 8.** Optical microscopic images of the morphology of Phthalcon 11 particle networks in epoxy composites cross-linked with different Jeffamine cross-linkers: (a) Jeffamine D230, (b) Jeffamine D400, and (c) Jeffamine D2000. Layer thickness  $\cong$  200 nm.



aggregates, and the average size of these building blocks may be the correlation length  $\xi$ , which is related to the  $\varphi$  and  $d_f$  for  $\varphi > \varphi_c$ :<sup>29,39–41</sup>

$$\xi \propto a\varphi^{1/(d_f-3)} \quad (6)$$

In (6),  $a$  is according to the theory the radius of a primary particle from which the fractal network is built. We assume that for our systems  $a$  is the radius of our small primary Phthalcon 11 aggregate.

For a fractal particle network placed between two electrodes the  $\sigma_v$  of the whole composite can be related to the fractal network structure according to (7):

$$\sigma_v = \frac{P}{R_p} \frac{l}{S} \propto \frac{a^{1+x}}{R_f} \xi^{-(2+x)} \quad (7)$$

$S$  is the contacting area of and  $l$  the distance between the electrodes,  $P$  is the number of conducting paths,  $R_p$  is the resistance of a single conducting path,  $R_f$  is the resistance of one particle aggregate plus the resistance between two contacting particle aggregates, and  $x$  is a constant with a value between 0 and 0.4. Equation 7 was easily deduced from the results of established theories.<sup>42</sup>

In this equation it is assumed that the  $\sigma_v$  of the polymer composite close to  $\varphi_c$  is related to the fractal morphology of the particle network through the parameter  $\xi$ . That means  $\sigma_v$  close to  $\varphi_c$  decreases when the correlation length increases. From the data presented in Figure 7 it may be concluded that the correlation length of the particle network increases when the molecular weight of the Jeffamine cross-linker used is enlarged. This was also suggested by the OM pictures (Figure 8). That the correlation length was larger was confirmed by analyzing the fractal network of the Phthalcon 11/epoxy layers cross-linked with Jeffamine 400 using the OM pictures and the approach described above of these materials (Jeffamine D400:  $\xi \approx 30 \mu\text{m}$ ;  $d_f = 1.61$ ; Jeffamine D230:  $\xi \approx 20 \mu\text{m}$ ;  $d_f = 1.75$ ). For these Jeffamine D400-cured materials we found that the layer thickness also influences the relation between  $\log \sigma_v$  and  $\varphi$  (see also above). These amazing differences could not be explained by published information. For both materials these Phthalcon 11 particle networks are formed during processing. Hence, the influence of the different Jeffamine cross-linkers on processing conditions was studied in more detail below.

**D. Influence of the Processing Conditions Used on the Fractal Particle Network Structure and on the  $\log \sigma_v$ – $\varphi$  Relation.** Before processing, the primary Phthalcon 11 particle aggregates are well dispersed in the component mixture, and the dispersion is stable under the experimental conditions chosen. Moreover, the viscosity and surface energy of these component mixtures are independent of the type of Jeffamine cross-linker used. During cross-linking these dispersions lose their colloidal stability due to the increased interfacial energy between the particles and the partly cross-linked matrix components and due to the evaporation of  $m$ -cresol. At the moment that the polymer matrix reaches its gel point, the viscosity of the system becomes so high that the (submicron) particle aggregates can hardly move any more. Hence, Phthalcon 11 particle network formation must occur before gelation.

Figure 9 shows the change in viscosity during cross-linking of the materials containing different Jeffamine cross-linkers. Taking the moment when the tangent of the loss angle ( $\tan \delta$ ) reaches 1 as the gel point, the gel points of these three coatings are 263, 325, and 610 s for respectively Jeffamine D230, D400, and D2000. The observed retardation of the gel point with

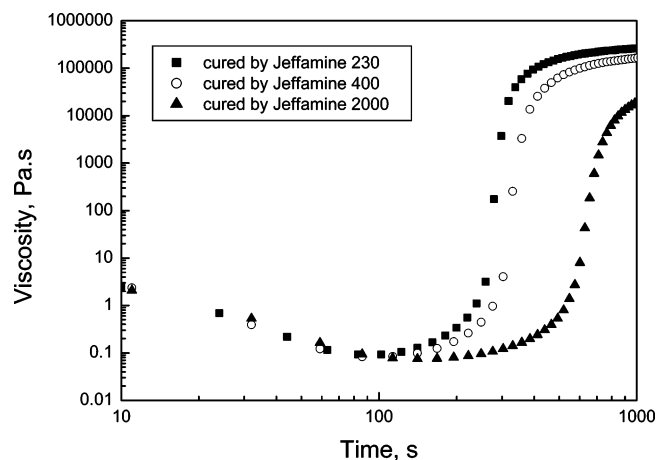


**Figure 9.** Viscosity evolution of 1.8 vol % Phthalcon 11/epoxy/Jeffamine/ $m$ -cresol mixtures during processing at 100 °C. The amount of  $m$ -cresol present in the prepolymer mixture before cure is the same.

increasing  $M_w$  of the cross-linker may be explained by a reduction in the concentration of amino and epoxy functional groups, which results in slower cross-linking rate. Consequently, by using a higher  $M_w$  cross-linker, the primary particle aggregates have more time to form larger secondary fractal aggregates with larger correlation lengths and smaller  $d_f$  (see eq 6), resulting in lower  $\sigma_v$  at a certain  $\varphi$ . These phenomena may also explain the variations observed in  $\varphi_c$ .

Other factors may also play a role in this process such as the influence of the evaporation of  $m$ -cresol and the catalytic effect of  $m$ -cresol on the cross-linking reaction. That the presence of  $m$ -cresol enhances the cross-linking reaction was observed in rheological experiments during cure at 100 °C using two similar Phthalcon 11/Epikote 828/Jeffamine D230 formulations. One of these also contains  $m$ -cresol and the other one not. In this last formulation Phthalcon 11 was dispersed directly in Jeffamine D230, and a gel point for this mixture of 2039 s was found, which is about a factor of 6 slower than for the other formulation containing  $m$ -cresol. The much earlier occurrence of the gel point in the presence of  $m$ -cresol can be explained by the weak acidity of  $m$ -cresol, which is known to act as a proton-donating catalyst in the primary amine–epoxy cross-linking reaction.<sup>43</sup> That indeed the influence of  $m$ -cresol already was large at the beginning of cure was also observed when formulations with and without  $m$ -cresol were studied at room temperature. Only for the mixtures with  $m$ -cresol non-Newtonian behavior and shear thinning were observed. This indicates a strong complexation of  $m$ -cresol with the epoxy and amino group as was proposed earlier for amine/epoxy/ $m$ -cresol mixtures.<sup>43</sup>

In the thin cross-linked Phthalcon 11/Jeffamine 230D/Epikote 828 layers made in the absence of  $m$ -cresol (method 1) fractal particle networks were also observed with OM. However, the  $\sigma_v$  of these layers could only be determined by using a noncontacting conductivity measuring method (Figure 10) because a thin insulating top layer was always formed,<sup>22</sup> as was confirmed by confocal scanning laser microscopy (see Experimental Section). Apparently, the larger Phthalcon 11 fractal aggregates present before cross-linking and the larger gel time stimulate sedimentation of the particle network during cross-linking.<sup>22</sup>

The time at which gelation occurs can be altered also by changing the cross-linking temperature. This was studied in more detail for cross-linked Jeffamine D230 layers made from Phthalcon 11 dispersions in  $m$ -cresol (method 2). At processing temperatures below 70 °C Phthalcon 11 particle networks were

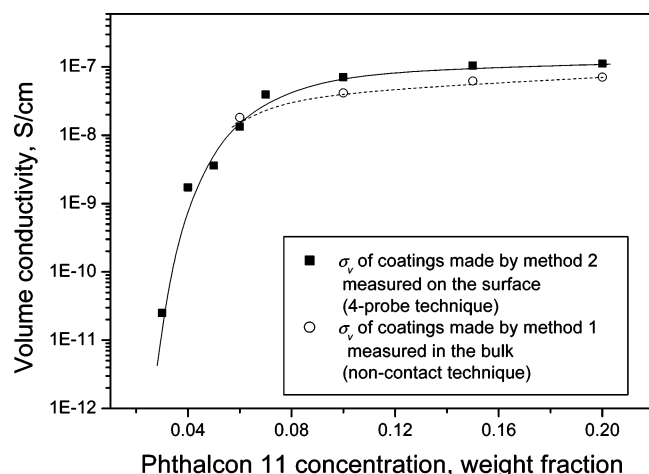


**Figure 10.** Volume conductivity of epoxy/Phthalcon 11 composite thin layers made by method 1 and method 2 measured by both four-probe and noncontact conductivity measurements. In method 1 Phthalcon 11 powder was dispersed directly in Jeffamine D230. In method 2 Phthalcon 11 powder was dispersed first in *m*-cresol (see Experimental Section).

found, but also an insulating top layer was formed. Rheological experiments showed that below this temperature the gel point increased above 2000 s. This is close to the value found for layers made without *m*-cresol at 100 °C (see above). In these layers always sedimentation was observed. At cross-linking temperatures above 120 °C no longer networks were formed, and the  $\sigma_v$  of the layers could not be measured any more. Rheological experiments showed that gelation occurred below 60 s. Apparently that is too short to finish Phthalcon particle network formation before the gel point.

Hence, the chosen processing conditions have also a major influence on the  $\log \sigma_v - \varphi$  and on the presence of a Phthalcon particle network after cross-linking. A complex relation exists between the processing method followed and the chosen components in the mixtures before processing. Rheological experiments confirm that the time available before the gel point of the polymer matrix is reached has been an important parameter in determining the presence of a particle network and insulating top layer in these materials.

#### E. Impact of Our Findings on Structure–Property Relations of Other Nanoparticle/Cross-Linked Polymer Matrices.

As has been shown above, the morphology and the  $\log \sigma_v - \varphi$  relation of thin cross-linked Phthalcon 11/epoxy layers are, apart from differences in interfacial energy between particles and matrix, also strongly influenced by small changes in the choice of prepolymer components used, the distribution of the nanoparticles in the dispersions before and during cross-linking, the processing temperature chosen for cross-linking, and the layer thickness. In our opinion this is not only important when Phthalcon 11 is used as nanofiller in combination with epoxy prepolymer and cross-linker. The models presented above to explain these results strongly suggest that these factors will have also a major impact on the particle morphology and the  $\log \sigma_v - \varphi$  relation of other (semi)conductive nanoparticle thermoset polymer matrix combinations. Apart from the particle dispersion quality and interfacial energy differences, most of the other factors mentioned above are neglected in publications on polymer thermoset materials containing (semi)conductive nanoparticles.<sup>1,2,9–12</sup> The data presented in this article show that this is likely to be incorrect especially when the amount of nanofiller present is well below 16 vol % and the layer thickness is small.

Quite often small amounts of nonconductive nanoparticles are used in thin cross-linked polymer matrices to enhance one or more properties such as modulus, impact resistance, scratch resistance, and gloss.<sup>1,44</sup> To realize an optimal enhancement of these material properties by the addition of these nanoparticles, the nanoparticles have to be dispersed well in advance through the polymer matrix. These nanoparticles have often a surface tension much larger than the components of the matrix itself. The results presented above as well as the results published before on Phthalcon 11 cross-linked epoxy thin layers<sup>22</sup> suggest that in these materials large particle aggregates and particle networks are likely to be present after cross-linking and that the ultimate particle morphology may depend in a similar way on interfacial energy differences between the particles and matrix components, layer thickness, processing conditions, and chosen matrix components as was found for the Phthalcon 11/epoxy materials described in this article. Publications about the thermoset composites containing nonconductive nanofillers generally neglect (part of) these aspects by explaining the relation between amount and type of filler used and the material properties realized for these composites.<sup>44,45</sup> This may also explain part of the contradictory results published by different groups and the lack of reproducibility often encountered when experiments are done to broaden the scope of a successful specific cross-linked nanoparticle polymer composite.

When thermoplastic polymers are used as matrix, the processing methods for preparing these composites are very different from those used for making thermoset thin layers, and we expect that the results reported above may not be applicable for those nanocomposites.

#### Conclusions

Phthalcon 11 crystals were used as nanosized semiconductive fillers in amine cross-linked epoxy materials. The  $\varphi_c$  of these materials may be below 1.0 vol %. This  $\varphi_c$  is much lower than the value derived from the statistical percolation approach, and the occurrence of such a low  $\varphi_c$  can be attributed to the formation of fractal particle networks from fractal particle aggregates. These fractal networks are likely to be formed by diffusion-limited cluster–cluster aggregation (DLA). Both OM and TEM pictures were used to determine the fractal morphology of the particle networks.

The  $\varphi_c$  and  $\sigma_v$  of the composites were found to be strongly dependent on the layer thickness. Values of  $\varphi_c$  between 9 vol % (thickness 9  $\mu\text{m}$ ) and 0.9 vol % (thickness 150  $\mu\text{m}$ ) were found. Modeling of the results showed that for bulk materials the  $\varphi_c$  can be as low as 0.55 vol %. This dependence can be quantitatively explained by a particle packing transition from 3-D to 2-D when the thickness of the composite decreases to a value comparable to the correlation length of the fractal particle networks.

The  $\log \sigma_v - \varphi$  also depends strongly on the cross-linker used to make the molecular networks. This is caused not only by the influence of the cross-linker on the interfacial energy between particles and matrix as was shown before<sup>22</sup> but also by the molecular weight of the diamine Jeffamine cross-linker used. These cross-linkers had the same surface tension, but the use of them led to a different Phthalcon 11 particle fractal network structure in the cured epoxy matrix. It was shown using rheological experiments that these differences could be explained by a change in cross-linking rate and gel time.

Also, the processing temperature used for making these Phthalcon 11/amine cross-linked epoxy layers had a major effect on the particle morphology of the cured layers and on the  $\log \sigma_v - \varphi$  relation of these layers.



Our results also suggest that, in general, for cross-linked polymer matrices containing other conductive or nonconductive nanoparticles large differences in material properties and morphologies of the cured materials may occur when the above-described modifications are introduced during the preparation of these materials. These effects were often neglected in studies on these materials.

**Acknowledgment.** We thank Dr. H. B. Brom and Ir. L. J. Huijbregts for their valuable comments on the manuscript, Mr. R. Sturme of Océ Technologies B.V. for his advice on non-contacting conductivity measurements and Dr. J. Laven for his advice on rheological measurements. This work forms part of the research program of the Dutch Polymer Institute (project 293).

## Appendix

In this Appendix it is discussed how the conductive properties of a layer might be influenced by the layer thickness. Consider a layer with a thickness  $H$  and a surface area  $L^2$ . The layer contains small conducting primary particles; each fractal particle has a radius  $a$ . These particles are converted into larger aggregates with a well-defined radius  $R$  via a DLA mechanism, which may depend on the layer thickness. The layer contains  $N$  such aggregates. We assume that the aggregates are purely randomly distributed throughout the layer and the volume conductivity of the layer is determined on the surface of the layer. Furthermore, only the case that the layer is thicker than or close to the aggregate dimensions,  $H \geq R$ , is considered. As a consequence, the cluster structures can be described with percolation models on a length scale  $\xi > R$  and with a DLA model for  $\xi < R$ . The effective volume percentage of aggregates  $p$  is given by

$$p \equiv \frac{4\pi R^3 N}{3HL^2} \times 100\% \quad (\text{A.1})$$

The aggregates are regarded as spheres with a radius  $R$ . In DLA the small particles form larger fractal aggregates, which can be characterized by a fractal dimension  $d_f$  ( $d_f < 3$ ). Therefore, the actual volume percentage of conducting particles  $\varphi$  is related to  $p$  via

$$\varphi = p \left( \frac{a}{R} \right)^{3-d_f} \quad (\text{A.2})$$

As already mentioned, the network of aggregates can be modeled with the help of percolation theory. The percolation variable that characterizes the problem is  $p$ . For  $H \rightarrow \infty$  a full system spanning network is formed above a threshold value  $p_c$ , which has a value around 15–17 vol % for impermeable spheres.<sup>8</sup>

The question that should be answered is, when does a layer conduct at all? Note that conduction parallel to the layer surface is meant. For an infinite system the answer is clear:  $p \geq p_c$ . In finite systems this inequality no longer holds: the percolation threshold  $p'_c$  will become a function of the  $H$ .

To find  $p'_c$ , we first subdivide the layer in “blobs” having a diameter  $H$ . Such blob is either conducting or nonconducting, which depends on the way that the aggregates are connected inside the blob. Let the number of conducting blobs be  $M$ . The percentage of the area covered by conducting blobs  $q$  can be defined as

$$q \equiv \pi M (H/2L)^2 \times 100\% \quad (\text{A.3})$$

Note that  $q$  is in fact the state variable for a 2D percolation problem. It is the probability that clusters of aggregates in this blob percolate. When  $H \rightarrow \infty$ , a full spanning network of conducting blobs can only be achieved for  $q \geq q_c$  (for nonoverlapping circles  $q_c \approx 45\%$ ).<sup>8</sup> The main task is now to relate the variable  $q$  with the experimental parameters  $a$ ,  $\varphi$ , and  $H$  via the variable  $p$ . Further, we define a second variable  $\Pi$ , which is the probability that a blob of size  $H$  is conducting, e.g., the probability that a blob contains a spanning network of conducting particles,  $0 \leq \Pi \leq 100\%$ . We have to remark that  $q = \kappa \Pi Z$ , where  $\kappa$  is a geometrical factor with a value close to unity. The variable  $\Pi$  obeys the following expression:<sup>29</sup>

$$\Pi = f[x] \equiv f[(p - p_c)(H/\lambda)^{1/\nu_3}] \quad (\text{A.4})$$

where  $\nu_3$  and  $\lambda$  are the correlation length exponent of 3D system ( $\nu_3 \sim 0.88$ ) and the typical size of the basic element (in our case  $\lambda = 2R$ ), respectively. An important property of  $\Pi$  is that it is a monotonously increasing function of  $x \equiv (p - p_c)(H/\lambda)^{1/\nu_3}$ .

The film will conduct current when it contains a spanning network of conducting blobs. This will be the case when  $\Pi$  exceeds a critical value  $\Pi_c$ . The percolation point  $\Pi = \Pi_c$  corresponds with a unique value of  $x = x_c$

$$x_c = (p'_c - p_c)(H/2R)^{1/\nu_3} \quad (\text{A.5})$$

Therefore, the percolation threshold of a layer with a thickness  $H$  obeys the following universal relationship

$$p'_c = p_c + x_c (H/2R)^{-1/\nu_3} \quad (\text{A.6})$$

When the layer thickness equals the aggregate diameter ( $H = 2R$ ),  $p'_c = \eta q_c$ , where  $\eta$  is a geometrical factor of order unity. This enables us to estimate the value of  $x_c$  as

$$x_c = \eta q_c - p_c \quad (\text{A.7})$$

By combination of the eqs 2 and 6, we can calculate the percolation threshold of a layer with thickness  $H$  in terms of real volume percentages:

$$\varphi_c = (a/R)^{3-d_f} p_c + 2^{1/\nu_3} x_c a^{3-d_f} R^{d_f+1/\nu_3-3} H^{-1/\nu_3} \quad (\text{A.8})$$

When a standard percolation process determines the structure of the aggregate network, we will observe  $\varphi_c \propto C + (H/2R)^{-1/\nu_3}$  ( $C$  is constant), and the data should converge to significant nonzero value equal to the bulk value,  $(a/R)^{3-d_f} p_c$ .

In the cross-linked Phthalcon 11/epoxy layers studied here, two fractal dimensions were observed at different scales of observation in the particle networks. Only one of these aggregate structures is comparable in size to the layer thickness. The other one is so small in respect to the layer thickness that it can be neglected in this model approach.

## References and Notes

- (1) (a) Othmer, K. *Encyclopedia of Chemical Technology*; John Wiley and Sons: New York, 1994/2000. (b) *Encyclopedia of Polymer Science and Technology*; John Wiley and Sons: New York, 2003.
- (2) (a) Skotheim, T.; Elsenbauer, R. L.; Reynolds, J. R. *Handbook of Conducting Polymers*, 2nd ed., revised and expanded; Marcel Dekker: New York, 1998. (b) Singh, N. *Handbook of Advanced Electronic and Photonic Materials*; Academic Press: London, 2001. (c) Chandrasekhar, P. *Conducting Polymers, Fundamental and Applications; A Practical Approach*; Kluwer Academic: Dordrecht, 1999. (d) Gul, V. E. *Structure and Properties of Conducting Polymer Composites*; CDV

- VSP: Utrecht, 1996. (e) Medalia, A. *Rubber Chem. Technol.* **1985**, 59, 433. (f) Sichel, K. *Carbon Black Polymer Composites*; Marcel Dekker: New York, 1982.
- (3) Zallen, R. In *The Physics of Amorphous Solids*; Wiley: New York, 1983; Chapter 4.
  - (4) Scarsbrick, R. M. *J. Phys. D: Appl. Phys.* **1973**, 6, 2098.
  - (5) Slupkowski, T. *Phys. Status Solidi* **1984**, A 83, 329.
  - (6) Yoshida, K. *J. Phys. Soc. Jpn.* **1990**, 59, 4087.
  - (7) Kirkpatrick, S. *Rev. Mod. Phys.* **1973**, 45, 574.
  - (8) Sahimi, M. *Applications of Percolation Theory*; Taylor and Francis: London, 1994.
  - (9) Levon, K.; Margolina, A.; Patashinsky, A. Z. *Macromolecules* **1993**, 26, 4061.
  - (10) Banerjee, P.; Mandal, B. M. *Macromolecules* **1995**, 28, 3940.
  - (11) (a) Brokken-Zijp, J. C. M.; Soloukhin, V. A.; Posthumus, W.; De With, G. *Athenes Conference on Coatings Science and Technology*; Proceedings 29, July 7–11, 2003, Vouliagmeni, Greece, p 49. (b) Brokken-Zijp, J. C. M.; Soloukhin, V. A.; Posthumus, W.; De With, G. *Prog. Org. Coat.*, in press.
  - (12) Sumita, M.; Sakata, K.; Asai, S.; Miyasaka, K.; Nakagawa, H. *Polym. Bull. (Berlin)* **1991**, 25, 265.
  - (13) Brokken-Zijp, J. C. M.; et al. Patents US 05319009, EP 0642547, EP 370586, and WO 09324562.
  - (14) Van der Putten, D.; Moonen, J. T.; Brom, H. B.; Brokken-Zijp, J. C. M.; Michels, M. A. J. *Phys. Rev. Lett.* **1992**, 69, 494.
  - (15) Adriaanse, L. J.; Reedijk, J. A.; Teunissen, P. A. A.; Brom, H. B.; Michels, M. A. J.; Brokken-Zijp, J. C. M. *Phys. Rev. Lett.* **1997**, 78, 1755.
  - (16) Lux, F. J. *Mater. Sci.* **1993**, 28, 285.
  - (17) Landauer, R. *J. Appl. Phys.* **1952**, 23, 779.
  - (18) McLachlan, D. S.; Blaszkiewicz, M.; Newnham, R. E. *J. Am. Ceram. Soc.* **1990**, 73, 2187.
  - (19) Soloukhin, V. A. Nanocomposite Hybrid Coatings on Polycarbonate. Ph.D. Thesis, Eindhoven University of Technology, 2003.
  - (20) Fournier, J.; Boiteux, G.; Seytre, G. *Phys. Rev. B* **1997**, 56, 5207.
  - (21) Aldissi, M. *Adv. Mater.* **1992**, 4, 368.
  - (22) Chen, Z.; Brokken-Zijp, J. C. M.; Michels, M. A. J. *J. Polym. Sci., Part B: Polym. Phys.* **2006**, 44, 33.
  - (23) Viswanathan, R.; Heaney, M. B. *Phys. Rev. Lett.* **1995**, 75, 24, 4433.
  - (24) Mandelbrot, B. B. *The Fractal Geometry of Nature*; Freeman: New York, 1982.
  - (25) Schüth, F.; Sing, K. S.; Weitkamp, W. J. *Handbook of Porous Solids*; Wiley-VCH: Weinheim, 2002; Vol. 1.
  - (26) Rothschild, W. G. *Fractals in Chemistry*; John Wiley & Sons: New York, 1998.
  - (27) Huijbregts, L. J.; Brom, H. B.; Brokken-Zijp, J. C. M.; Michels, M. A. J.; de Goeje, M.; Yuan, M. *Phys. Status Solidi C* **2006**, 3, 259.
  - (28) Brokken-Zijp, J. C. M.; Chen, Z. *Synthesis and Structure of Novel Aquocyanophthalocyaninato Cobalt (III) Semiconductor and Its Applications in Conductive Polymer Composites*, to be published.
  - (29) Stauffer, D.; Aharony, A. *Introduction to Percolation Theory*, 2nd ed.; Taylor & Francis: London, 1992.
  - (30) Clerc, J. P.; Giraud, G.; Laugier, J. M.; Luck, J. M. *J. Phys. A* **1985**, 18, 2565.
  - (31) Heaney, M. B. *Phys. Rev. B* **1995**, 52, 12477.
  - (32) Weitz, D. A.; Huang, J. S.; Lin, M. Y.; Sung, J. *Phys. Rev. Lett.* **1984**, 53, 1657.
  - (33) Brady, R.; Ball, R. C. *Nature (London)* **1984**, 309, 225.
  - (34) Vermant, J.; Solomon, M. J. *J. Phys.: Condens. Matter* **2005**, 17, R187.
  - (35) Meakin, P. J. *Phys. Rev. A* **1983**, 27, 1495.
  - (36) Jullien, R. *Contemp. Phys.* **1988**, 28, 477.
  - (37) Barber, M. N. *Phase Transitions and Critical Phenomena*; Academic Press: New York, 1983; Vol. 8, p 145.
  - (38) Roldughin, V. I.; Vysotskii, V. V. *Prog. Org. Coat.* **2000**, 39, 81.
  - (39) Bremer, L. Fractal Aggregation in Relation to Formation and Properties of Particle Gels. Doctoral Thesis, LU Wageningen, 1992.
  - (40) Posthumus, W. UV-curable Acrylate Metal Oxide Nanocomposite Coatings. Doctoral thesis, Eindhoven University of Technology, 2004.
  - (41) Shih, W. H.; Shih, W. Y.; Kim, S. I.; Liu, J.; Aksay, I. A. *Phys. Rev. A* **1990**, 42, 4772.
  - (42) Bunde, A.; Havlin, S. *Fractals and Disordered Systems*, 2nd revised and enlarged; Springer: Berlin, 1996; Chapter 3.
  - (43) Lee, H.; Neville, K. *Handbook of Epoxy Resins*; McGraw-Hill: London, 1982.
  - (44) For instance: (a) Liu, H.; Zheng, S.; Nie, K. *Macromolecules* **2005**, 38, 5088. (b) Nicolais, L.; Larotenuto, G. *Metal–Polymer Nanocomposites*; Wiley: New York, 2004. (c) Friedrich, K.; Zhong Zhang; Schlarb, A. K. *Compos. Sci. Technol.* **2005**, 65, 2329. (d) Thostenson, E. T.; Li, C.; Chou, T.-W. *Compos. Sci. Technol.* **2005**, 65, 491. (e) Buryachenko, V. A.; Roy, A.; Lafdi, K.; Anderson, K. L.; Chellapilla, S. *Compos. Sci. Technol.* **2005**, 65, 2435. (f) Chiang, H.-W.; Chung, C.-L.; Chen, L.-C.; Li, Y.; Wong, C. P.; Fu, S.-L. *J. Adhes. Sci. Technol.* **2005**, 19, 565. (g) Lange, J.; Wyser, Y. *Packag. Technol. Sci.* **2003**, 16, 149. (h) Chen, B.; Evans, R. G. E. *Macromolecules* **2006**, 39, 1790.
  - (45) Soloukhin, V. A.; Posthumus, W.; Brokken-Zijp, J. C. M.; Loos, J.; de With, G. *Polymer* **2002**, 43, 6169 and literature quoted there.

MA052144+